(27) J. K. Burdett, R. C. Fay, and R. Hoffmann, *Inorg. Chem.*, **17**, 2553 (1978).
(28) J. K. Burdett, *Struct. Bonding (Berlin)*, **31**, 67 (1976).
(29) S. F. A. Kettle, *Spectrochim. Acta*, **22**, 1388 (1966).
(30) These values are for d^{10} tetrahedral systems, e.g., $Ni(CO)_3L$, and low-spin d^8 trigonal-bipyramidal cases, e.g., $Fe(CO)_4L$, where all of the d_π orbitals are filled. Deviations from the additivity scheme might be expected for electronic configurations with fewer d electrons. Octahedral d^5 species appear to be aberrant. Tetrahedral d^6 species, e.g., $CpMn(CO)_3$, fit well in the scheme. Here the molecular orbital structure is pseudooctahedral with three low-lying d_π-type orbitals filled.
(31) D. W. Smith, *J. Chem. Soc., Dalton Trans.*, 834 (1976).
(32) J. K. Burdett, *Inorg. Chem.*, **14**, 375 (1975).
(33) R. N. Perutz and J. J. Turner, *J. Am. Chem. Soc.*, **97**, 4800 (1975).
(34) Y. W. Yared, S. L. Miles, R. Bau, and C. A. Reed, *J. Am. Chem. Soc.*, **99**, 7076 (1977).
(35) A. R. Rossi and R. Hoffmann, *Inorg. Chem.*, **14**, 305 (1975).
(36) In both case (ii) and case (iii) although the nonbonding orbital contributes nothing overall to the stabilization of the MLL′ unit in general, it will contain a small amount of central-atom character which will lead to some weakening of one bond and strengthening of the other. The overall result (see ref 2a for a discussion of this point for π-bonded systems) gives very similar trends in the ML and ML′ bond overlap populations as a function of the H_{ii} and S_{ij} as eq 22 shows for the bond-stabilization energies and reinforces this effect.
(37) This is reached by an obvious algebraical division of the cross terms in eq 22 between ML and ML′. If the cross terms are divided equally, then the relevant equation becomes

$$2\frac{S_\sigma^2}{(\Delta\epsilon)^2}\left[\frac{S_\sigma^2}{\Delta\epsilon}-\frac{S_\sigma'^2}{\Delta\epsilon'}\frac{\frac{1}{2}(\Delta\epsilon+\Delta\epsilon')}{\Delta\epsilon'}\right]$$

(38) (a) R. McWeeney, R. Mason, and A. D. C. Towl, *Discuss. Faraday Soc.*, **47**, 20 (1969); (b) R. Mason and A. D. C. Towl, *J. Chem. Soc. A*, 1001 (1970).
(39) R. G. Pearson, *Inorg. Chem.*, **12**, 712 (1973).
(40) The perturbation formalism used was that developed by A. Imamura, *Mol. Phys.*, **15**, 225 (1968). The M–H distances were set at 2.1 Å and Cr parameters were taken for the metal: T. A. Albright, P. Hofmann, and R. Hoffmann, *J. Am. Chem. Soc.*, **99**, 7546 (1977).
(41) The S–H bond lengths were fixed at 1.4 Å and the H_{ii} of the perturbed hydride ligand was lowered to −14.6 eV. All other parameters used in the calculation were taken from R. Hoffmann, H. Fujimoto, J. R. Swenson, and C.-C. Wan, *J. Am. Chem. Soc.*, **95**, 7644 (1973). No d orbitals were included on sulfur.
(42) If 3d orbitals on sulfur are included with parameters (see ref 41 for details) that allow for unrealistically large interactions, then while the cis S–H overlap population on going from SH_6 to SH_5X is increased very slightly, the trans one stays approximately constant. This is a consequence of mixing a low-lying e_g component, mainly 3d in character and antibonding to hydrogen, into one component of the $1t_{1u}$ set. This is precisely the factor which dominated in our discussion of ML_6 complexes where metal d-ligand overlap forms a major part of the bonding.
(43) E. M. Shustorovich and Yu. A. Buslaev, *Inorg. Chem.*, **15**, 1142 (1976); E. M. Shustorovich, *Zh. Strukt. Khim.*, **15**, 123, 977 (1974); *J. Am. Chem. Soc.*, **100**, 7513 (1978); **101**, 792 (1979); *Inorg. Chem.*, **17**, 2648 (1978), and references therein; N. A. Popov, *Koord, Khim.*, **1**, 731 (1975); **2**, 1155, 1340 (1976).
(44) J. M. Howell, *J. Am. Chem. Soc.*, **97**, 3930 (1975).
(45) Y. A. K. Syrkin, *Izv. Akad. Nauk SSSR, Otd. Ser. Khim.*, 69 (1948).
(46) J. K. Burdett, *Inorg. Chem.*, **18**, 1024 (1979).
(47) B. M. Gimarc, *J. Am. Chem. Soc.*, **92**, 266 (1970).

Contribution from the Department of Chemistry,
University of Rochester, Rochester, New York 14627

Metalloporphyrin–Ligand Equilibria: A Ligand Field Rationale

GEORGE McLENDON* and MARK BAILEY

Received November 2, 1978

Equilibrium constants for the reaction PM–OH_2 ⇄ PM–OH (K_{OH}) are reported where P = tetraphenylporphyrinsulfonate or hematoporphyrin and M = Cr(III), Mn(III), Fe(III), Co(III), or Rh(III). The observed trends in the binding constants may be explained by a simple electrostatic (ligand field) model. For a tetragonal field, the calculated effective charge along the z axis is shown to correlate with the binding constant of axial OH^-. Similar trends are observed for imidazole binding to metalloporphyrins. It is found that the magnitude of the equilibrium constants is surprisingly independent of the nature of the porphyrin substituents. Finally, the relationship between these trends in axial bonding and heme protein conformational energy is briefly discussed.

Introduction

The reactions of ligands with metalloporphyrins have long been of active interest to both biochemists and coordination chemists.[1] However, this interest has not yet translated into a general understanding of the factors which control metalloporphyrin–ligand equilibria (and kinetics).[2]

To understand the general trends in such bonding, two limiting approaches might be taken. The first treats metalloporphyrins by using a tetragonally distorted ligand field model, so that some molecular orbitals may be designated as clearly metal centered. The occupancy of these orbitals would thereby influence the strength of metal–ligand interaction. In this approach, porphyrins are treated much the same as other ligands (e.g., simple amines) and constructs of formal metal oxidation states retain some significance (e.g., $[CoTPPS_4]^{3-}$[27] may be treated as a "d^6 Co(III)" complex).

By contrast, it is often argued in the extensive porphyrin literature that metal–ligand orbital mixing is so extensive that the concept of metal centered MO's loses significance.[2-6] For example it has been noted that there is a "necessity to choose a strongly delocalized model of electronic configuration of the complex compared to the usual metal centered description".[6] Others have argued in a similar vein that orbital mixing is so complete in metalloporphyrins that assignment of electrons to metal-centered orbitals and concurrent assignment of formal oxidations states is invalid.[5,7] Previous investigations of ligand equilibria of metalloporphyrins have been limited to a single metal with a single type of porphyrin.[3-9] Thus cross comparisons could not apparently be made between, e.g., CoTPPS and FeHMP. In this case, trends in metalloporphyrin ligand equilibria would not be easily discerned.

In order to test these limiting models, we have determined ligation (hydrolysis) equilibria constants

$$MPOH_2 \overset{K_{OH}}{\rightleftharpoons} MPOH + H^+$$

for a series of metalloporphyrins MP where M = Cr(III), Mn(III), Fe(III), Co(III), or Rh(III) and P = tetraphenylporphinesulfonate (TPPS) or hematoporphyrin (HMP). More limited data for metal–imidazole binding are also reported. The results are shown to be semiquantitatively explained by a simple electrostatic model. Finally, the implications of these results for heme protein chemistry are briefly discussed.

Experimental Section

Materials. Ligands. Hematoporphyrin free base was purchased from Sigma Chemicals. TPP and TPPS[27] were synthesized and purified by standard procedures.[1,16] All metal salts and metal carbonyls were reagent grade, purchased from Alfa. Water was doubly distilled and deionized.

0020-1669/79/1318-2120$01.00/0

Table I. Metalloporphyrin Hydrolysis Equilibrium Data[a]

M	pK_{OH}[b]	$pK_{(OH)2}$[c]	ref
M-$TPPS_4$			
Cr(III)	4.7 ± 0.1 (4.6)	7.6 ± 0.1	this work (cf. ref 6)
Mn(III)	11.8 ± 0.2		this work
Fe(III)	8.1 ± 0.3 (overlaps with dimer)	7.9	this work (cf. ref 3)
Co(III)	5.8 ± 0.1	11.0 ± 0.1	this work
Rh(III)	6.8 ± 0.1 (7.4)		this work (cf. ref 9)
M-HMP			
Cr(III)	5.2 ± 0.1	7.8 ± 0.1	this work
Mn(III)	(11.2 ± 0.1)		10
Fe(III)	8.0 ± 0.6 (overlaps with dimer)		this work
Co(III)	5.4 ± 0.4		this work
Rh(III)	5.1 ± 0.1		this work

[a] H_2O solution, 25.0 °C, $\mu = 0.1$ M KNO_3; values in parentheses refer to available literature values. [b] $MPOH_2 \rightleftarrows MP\text{-}OH + H^+$ (K_{OH}). [c] $MPOH \rightleftarrows MP(OH)_2 + H^+$ ($K_{(OH)2}$).

Table II. Metalloporphyrin + Imidazole Equilibrium Data[a]

M	pK_{Im}	ref
$Cr^{III}HMP$	6.6 ± 0.1	this work
$Mn^{III}HMP$	0.1 ± 0.1	this work
$Fe^{III}HMP$	5.3[b]	this work
$Cr^{III}TPP$	6.4 (acetone)	11
$Fe^{III}TPP$	3.9 (benzene)	12
$Fe^{III}DP$[c]	3.4	

[a] MeOH, 25.0 °C except where noted. [b] Disproportionates. [c] DP = deuteroporphyrin.

Metalloporphyrins. (A) Fe(III), Co(III), Cr(III), Mn(III). The basic method of Adler was used.[15] Free base porphyrin was reacted with M(II) chloride ($CrCl_2$, $CoCl_2 \cdot 6H_2O$) or acetate ($Mn(C_2H_3O_2)_2$, $Fe(C_2H_3O_2)$) in stoichiometric proportion in refluxing DMF under N_2 atmosphere. Reaction progress was monitored by visible spectroscopy at ca. 10-min intervals. If reaction was incomplete, approximately 15% excess metal was added. This procedure was repeated until no free porphyrin remained. Addition of two volumes of water at ice temperature led to precipitation of product.

(B) Rh, Ru. Porphyrin and metal carbonyl ($(Rh(CO)_2Cl)_2Ru_3CO_{12}$) were reacted in glacial acetic acid under N_2 atmosphere. Workup followed the methods of Tsutsui.[16] ClRhP(CO) was reacted with 1 M KOH to displace CO and Cl. All products were purified by column chromatography by using alumina or polyamide (Beckmann cc 6.6) columns.

Products were verified by visible spectroscopy, IR spectra, and elemental analysis. Both spectra and analyses were satisfactory.

Methods. pK values and imidazole equilibria were determined by spectrophotometric titration by using a Cary 118 spectrometer. Temperature was maintained at 25.0 °C. Experiments were performed both batchwise and stepwise. Any initial precipitation in the stock solutions was removed by membrane filtration (Gelman).

Data were analyzed by the method of Rose and Drago.[26]

Results and Discussion

The results of the present investigations combined with available comparative data from a literature survey of previous work are contained in Tables I and II. Some comment as to the accuracy of the results is of course necessary. In cases where literature data were repeated, our values are in excellent agreement with previous reports (Table I). In general, the hematoporphyrin values are far less reliable than the TPPS one, probably due to the poorer solubility of the former at pH <5. Nonetheless, the same general trends are apparent in both cases. There are some inconsistencies among various literature reports, particularly for iron and cobalt porphyrins. In these cases, our data fall in the middle of the reported ranges. These inconsistencies probably derive from medium effects, since we have found a strong ionic strength (and some specific electrolyte) dependence of the hydrolysis equilibria. All equilibria reported showed smooth titration curves which were highly reproducible.

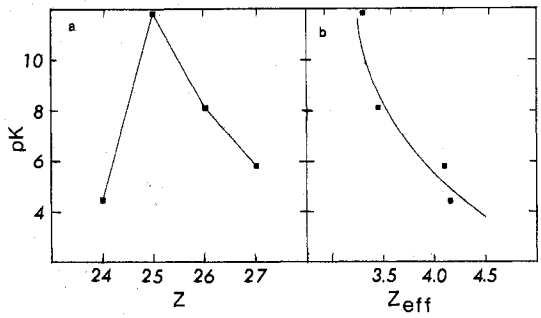

Figure 1. (a) Plot of metalloporphyrin hydrolytic equilibrium constant (pK_{OH}) vs. metal atomic number. Data are from Table I. All data refer to 25.0 °C, $\mu = 0.1$ M (KNO_3). (b) Plot of metalloporphyrin hydrolytic equilibrium constants vs. effective charge along the z axis (Z_{eff}) calculated as described in the text.

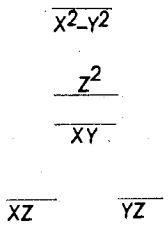

Figure 2. Relative d orbital energies in a tetragonal field of a metalloporphyrin.

We were concerned with possible porphyrin aggregation. Thus the equilibria were determined at several porphyrin concentrations, without effect on the spectra or derived thermodynamic parameters; 5×10^{-6} M was the concentration used for the remainder of the investigation. Thus if aggregation does occur, it does not seem to affect the equilibria studied here. An exception is provided by Fe(III), where the concentration of μ-oxo species increased with the increasing concentration. This overlapping dimerization leads to a particularly high uncertainty for the pK_{OH} of Fe(III).

A surprising finding of the investigation was the relative insensitivity of the ligation equilibria to the particular type of porphyrin system investigated. This is most clearly shown in the imidazole binding results, where the binding constant for CrHMP + Im is very close to the reported binding constant for CrTPP + Im. These relatively small changes in equilibria are markedly contrasted by kinetic results, which show large effects of porphyrin structure on the rate of axial ligand exchange.[17-20] Clearly these kinetic effects must operate to a similar degree in both the forward and reverse directions. That is to say, the energies of both the reactant and product are (relatively) unchanged while the transition state is stabilized.

The relative magnitudes of the hydrolytic equilibria (and imidazole bonding) do not follow a simple Irving–Williams order,[13] as shown in Figure 1a. They further cannot be simply correlated with quantum mechanically calculated charges on the central metals.[14]

What then is responsible for these trends? In a limiting electrostatic (ligand field) model outlined above, the metal orbitals would follow the general ordering given in Figure 2. As the metal electron configuration changed, so would the occupancy of "d orbitals" directed along the z axis, where the ligand adds.

In this electrostatic model, repulsion between these d electrons and the incoming ligand electron pair should play a large role in determining the metal–ligand affinity. This simple concept may be more quantitatively approached in the

Table III. Structural Data for Selected Metalloporphyrins[a]

MP	axial ligand	d_{z^2} occupancy	axial bond, Å
$[FeTPP(Im)_2]^+$	Im	–	1.97
$[CoTPP(Im)_2]^+$	Im	–	1.93
[MnTPPPyCl]	Py	+	2.44
$[NiTPyP(Im)_2]$	Im	–	2.16
[ZnTPyP(Py)]	Py	+	2.15
$[FeTPP(MeIm)_2]$	Im	–	1.99

[a] See ref 22 for specific literature references for individual structures.

following way. Consider the additional shielding (above normal Slater shielding) along the z axis induced by d_{z^2}, d_{xz}, and d_{yz} occupancy. In a simple approach to account for this directed electron repulsion, a shielding value of 1.0 is assigned to a d_{z^2} occupancy while 0.5 is used for electrons in the d_{xz} and d_{yz} orbitals, yielding an effective charge expression of the form

$$Z_{eff} = Z - (Z_{Slater} + (1)nd_{z^2} + (0.5)n'd_{xz,d_{yz}})$$

n, n' being the occupancy status of the indicated orbitals. Although more exacting approximations could be used, this is only an approximation intended to illustrate a trend. The approximation should be fairly constant through the transition-metal series used in this report. When this charge is plotted against the measured hydrolysis equilibria for the various metal derivatives, a clear relation (in form of a smooth curve) may be seen. Far less data are available for imidazole binding, due to problems of disproportionation. However, the relative affinities of Cr(III), Mn(III), and Fe(III) follow the expected trend from Z_{eff}.

These observations strongly suggest that metalloporphyrin electronic structure, and the coupling of that electronic structure to porphyrin equilibria, is much simpler than is generally appreciated. The data cannot be easily rationalized from quantum mechanical results, at present levels of calculation, but are clearly explained in terms of a simple crystal field model. Indeed, in retrospect, it is clear that metal–porphyrin mixing could *not* be extremely extensive for these specific metals since such extensive mixing would inevitably lead to large separations of the molecular orbitals and metalloporphyrins would always be low spin.[21] In sum, one must be cautious to avoid confusing a highly delocalized ligand with a delocalized metal–ligand system.

The dynamic properties we have noted have clear structural counterparts.

The relationship between electronic and physical structure has been dealt with in detail by Scheidt in a recent review.[22] In cases where d_{z^2} is occupied (and ligand affinity low) long axial bond lengths are also observed (Table III).

It should be noted that the previous suggestions of metal–porphyrin delocalization were based on the clear observations that metalloporphyrins were far more labile toward ligand exchange than analogous metal–amine complexes.[6,7,17-20] Thus, while simple cobalt(III) and chromium(III) amines are inert, cobalt(III) and chromium(III) porphyrins are not.[6,7,17] This lability could, of course, arise from destabilization of the ground state (by orbital mixing) or stabilization of the excited state. It seems clear that the latter occurs. As discussed in detail by Pasternak,[18] porphyrins might be expected to strongly stabilize the five-coordinate intermediate formed in the dissociative ligand exchange, thereby increasing the rate of reaction but leaving the equilibria essentially unchanged.

Relation to Heme Proteins

Finally, the implications of these results for metalloporphyrin–protein interaction in heme proteins should be briefly mentioned. In studies of metal-centered effects on heme

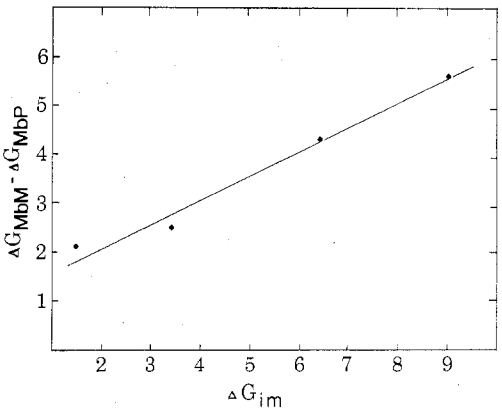

Figure 3. Plot of total conformational free energy of metal-substituted myoglobins determined by the methods in ref 23 vs. the free energy of metal porphyrin–imidazole bonding.

Table IV. Dependence of Heme–Protein Conformational Energy on Imidazole Bond Energy

MMb	$\Delta G_{conform}$[a]	ΔG^{Imb}
$Cr^{III}Mb$	5.6	8.0
$Mn^{III}Mb$	2.1	0.5
$Fe^{III}Mb$ high spin	2.5	2.4
$Fe^{III}Mb$ low spin	4.3	5.4

[a] See ref 23 and 24 for a discussion of conformational free energy. [b] From Table II.

protein conformation, a clear correlation between metal–imidazole bond strength and overall protein conformational free energy, measured independently, has been found (Table IV, Figure 3). These results are discussed in detail elsewhere.[23,24] Thus, the common (Perutz type) mechanisms[25] which focus on the role of metal spin state in changing protein conformation (or, more correctly, conformational free energy) have a clear thermodynamic basis in the dependence of the metal imidazole bonding strength.

Registry No. Cr(III)-$TPPS_4$-OH_2, 33339-70-7; Mn(III)-TPP-S_4-OH_2, 70288-07-2; Fe(III)-$TPPS_4$-OH_2, 70288-08-3; Co(III)-$TPPS_4$-OH_2, 58881-09-7; Rh(III)-$TPPS_4$-OH_2, 66035-54-9; Cr(III)-HMP-OH_2, 70288-09-4; Mn(III)-HMP-OH_2, 70288-10-7; Fe(III)-HMP-OH_2, 70288-11-8; Co(III)-HMP-OH_2, 70288-12-9; Rh(III)-HMP-OH_2, 70288-13-0; Cr(III)-HMP-Im, 70288-14-1; Mn(III)-HMP-Im, 70288-15-2; Fe(III)-HMP-Im, 70288-16-3.

References and Notes

(1) K. M. Smith, Ed., "Porphyrins and Metalloporphyrins", Elsevier, New York, 1975.
(2) P. Hambright, ref 1.
(3) E. Fleischer, J. Palmer, T. Srivastava, and A. Chatterjee, *J. Am. Chem. Soc.*, **93**, 3162 (1971).
(4) R. Pasternak and G. Parr, *Inorg. Chem.*, **15**, 3087 (1976).
(5) G. Kolski and R. Plane, *J. Am. Chem. Soc.*, **94**, 3740 (1972).
(6) E. Fleischer and M. Krishnamurthy, *J. Coord. Chem.*, **2**, 89 (1972).
(7) E. Fleischer and M. Krishnamurthy, *J. Am. Chem. Soc.*, **93**, 3784 (1971).
(8) R. Pasternak and M. Cobb, *J. Inorg. Nucl. Chem.*, **35**, 4327 (1973).
(9) M. Krishnamurthy, *Inorg. Chim. Acta*, **25**, 215 (1977).
(10) P. Loach and M. Calvin, *Biochemistry*, **2**, 361 (1963).
(11) G. Sommerville and F. Basolo, *J. Am. Chem. Soc.*, in press.
(12) P. Brault and J. Rougee, *Biochem. Biophys. Res. Commun.*, **57**, 654 (1974).
(13) F. A. Cotton and G. Wilkinson, "Advanced Inorganic Chemistry", Wiley, New York, 1972.
(14) M. Gouterman, L. Hanson, G. Khalil, W. Leenstra, and J. Buchler, *J. Chem. Phys.*, **62**, 2343 (1975).
(15) A. Adler, F. Longo, F. Kampas, and J. Kim, *J. Inorg. Nucl. Chem.*, **32**, 2443 (1970).
(16) M. Tsutsui and G. Taylor, ref 1, p 282.
(17) T. Yonetani, *J. Biol. Chem.*, **243**, 4715 (1972).
(18) R. Pasternak, M. Cobb, and N. Sutin, *Inorg. Chem.*, **14**, 866 (1975).
(19) R. Pasternak and J. Stahlbusch, *J. Chem. Soc., Chem. Commun.*, 106 (1977).
(20) W. Randall and R. Alberty, *Biochemistry*, **6**, 1520 (1967).
(21) M. B. Hall, personal communication. We are grateful to Professor Hall for this suggestion.

(22) W. R. Scheidt, *Acc. Chem. Res.*, **10**, 339 (1977).
(23) G. McLendon and K. Sandberg, *J. Biol. Chem.*, **253**, 3913 (1978).
(24) G. McLendon and P. Murphy, *J. Biol. Chem.*, submitted for publication.
(25) M. Perutz, *Brit. Med. Bull.*, **32**, 315 (1976).
(26) R. Drago, "Physical Methods in Chemistry", Reinhold, New York, 1976.
(27) Abbreviations: HMP = hematoporphyrin, $TPPS_4$ = tetraphenylporphyrinsulfonate, TPP = tetraphenylporphyrin, TPyP = tetrapyridylporphyrin.

Contribution from the Department of Chemistry, The University of Mississippi, University, Mississippi 38677

Lower Valence Fluorides of Vanadium. 3. Structures of the Pseudohexagonal A_xVF_3 Phases (Where A = K, Rb, Tl, or Cs)

Y. S. HONG, R. F. WILLIAMSON, and W. O. J. BOO*

Received December 27, 1978

Hexagonal tungsten bronze like A_xVF_3 compounds (A = K, Rb, Tl, or Cs) were prepared and their structures studied by using polarized microscopy and X-ray diffraction techniques. Superlattice reflections were observed on Debye–Scherrer films which made the *a* dimensions of A_xVF_3 twice those of A_xWO_3. Relative intensities of these reflections suggest ordering of A^+ ions in partially filled sites. Weissenberg and Guinier–Hägg photographs revealed that K_xVF_3, Rb_xVF_3, and Tl_xVF_3 are distorted slightly from hexagonal and are orthorhombic. The distortion ratio $|a|/3^{1/2}|b|$ demonstrates the magnitude and direction of the distortion, and for lower values of x, it is approximately 1.005. For samples of composition $Rb_{0.32}VF_3$ and $Tl_{0.30}VF_3$ (x is near its maximum theoretical value $^1/_3$), the direction of the distortion is reversed, and the distortion ratios found were 0.996 and 0.991, respectively. Typical lattice constants: for $K_{0.25}VF_3$ a = 12.895, b = 7.398, and c = 7.533 Å; for $Rb_{0.25}VF_3$ a = 12.904, b = 7.411, and c 7.550 Å; for $Tl_{0.25}VF_3$ a = 12.928, b = 7.427, and c = 7.563 Å; for $Rb_{0.32}VF_3$ a = 12.874, b = 7.464, and c = 7.567 Å; for $Tl_{0.30}VF_3$ a = 12.841, b = 7.479, and c = 7.572 Å. These orthorhombic compounds form domains which are oriented 120° with respect to each other giving a macroscopic effect of hexagonal symmetry. X-ray photographs of Cs_xVF_3 compounds display weak superlattice reflections; however, no distortion from hexagonal symmetry was observed. The lattice constants of this phase increase slightly with x.

Introduction

Hexagonal structures, similar to the Magnéli tungsten bronzes (A_xWO_3),[1] have been reported for first-row transition-metal fluorides of the general formula $A_xM^{II}{}_xM^{III}{}_{1-x}F_3$ (A_xMF_3), where x has the maximum theoretical value of $^1/_3$, A = K, Rb, Cs, or Tl, and M = Fe,[2] Cr,[3] or V.[4] The bronze structure ($P6_3/mcm$) may be described as a rigid lattice of WO_3 units having parallel tunnels of hexagonal cross section. These tunnels provide sites for the monovalent ion whose size and relative number affect crystallographic dimensions.

In the bronze structures, there is not only the atomic ordering of the parent WO_3 lattice but also the possibility of ordering within tunnels. The latter offers an explanation for the superlattices observed in tetragonal bronze structures by early investigators.[5] More recently, ordering within tunnels has been substantiated by lattice-imaging electron microscopy in both hexagonal and tetragonal tungsten bronzes. Hexagonal K_xWO_3,[6] studied by this technique, revealed clusters of empty tunnels which appeared randomized with no apparent long-range ordering. This qualifies the system as being truly nonstoichiometric. Atomic ordering in the tetragonal bronze-like region of the Nb_2O_5–WO_3[7-9] system consists of empty or filled pentagonal tunnels which exhibit two-dimensional ordering in a variety of patterns. Resultant phases of different stoichiometry possess characteristic superlattices and in some instances give rise to domain structures.

Neither superstructures nor domains have been previously reported for materials having hexagonal tungsten bronze like structures. Both have been found in the A_xVF_3 systems. This paper reports these structures from X-ray diffraction results aided by polarized microscopy.

Experimental Section

Sample preparation consisted of vacuum encapsulating appropriate quantities of thoroughly mixed alkali fluoride, VF_2, and VF_3 inside 0.64-cm diameter by 3.2-cm long Mo capsules by using electron-beam welding techniques. VF_2 and VF_3 were prepared from 99.9% V metal, as previously described by Stout and Boo.[10] Optical grade KF, RbF, and CsF were obtained commercially along with 99.9% TlF. All handling and transferring of starting materials were carried out inside an inert-atmosphere glovebox. The sealed capsules were fired in a vacuum furnace at 800 °C. Formation of the hexagonal-like phases was found to be complete in 30 h, but to ensure equilibrium, all samples were heated for 30 days. Weight checks were made on capsules following each step of the procedure.

Products were examined by stereoscopic and polarized microscopy. Limiting values of x in the A_xVF_3 phases were determined from two-phase samples (except in the case of $K_{0.27}VF_3$ where a trace of a third phase was present and in $Tl_{0.30}VF_3$ where considerable oxidation–reduction occurred between Tl^+ and V^{2+}). When possible, these phases were separated by Pasteur's method and their compositions determined by chemical analyses. When phases could not be satisfactorily separated, compositions were estimated from relative amounts of phases present as observed by optical microscopy or measured by X-ray powder methods. Pseudohexagonal symmetry of $K_{0.25}VF_3$ was determined from Weissenberg photographs by using Cu Kα and Fe Kα radiation in conjunction with Guinier–Hägg results. Guinier–Hägg data were taken with Cu Kα_1 and Cr Kα_1 radiation and refined by least squares. Elemental analyses of products were obtained commercially.

Results

Hexagonal-like A_xVF_3 phases were studied in which x had minimum, intermediate, and maximum values. Sample compositions prepared and products formed are given in Table I. Tiny needle-shaped crystals were obtained from $K_{0.25}VF_3$.

Polarized Microscopy. The hexagonal-like A_xVF_3 phases were formed in every sample and were easily identified by polarized microscopy. They are optically dense and their transmitted color is brownish red. When viewed between crossed nicols, they appear weakly birefringent. By contrast, both tetragonal and orthorhombic phases of the KF–VF_2–VF_3 system (previously described in this series[11]) are less optically dense, brighter red, and moderately birefringent. Transmitted colors of the modified pyrochlores $Rb_{0.50}VF_3$ and $Cs_{0.50}VF_3$ are also brighter red but are optically dense and weakly birefringent.

X-ray Diffraction. K_xVF_3. Laue symmetry 6*mm* was exhibited by low-angle reflections on (*hkin*) Weissenberg photographs of $K_{0.25}VF_3$ single crystals. Low-angle reflections on even-layer films (n = 0, 2, or 4) resembled those of hexagonal tungsten bronzes;[1] however, weak reflections found on odd-layer films (n = 1 or 3) doubled the *a* dimension.

0020-1669/79/1318-2123$01.00/0